RAB18 is a key regulator of GalNAc-conjugated siRNA-induced silencing in Hep3B cells

Jiamiao Lu,[1] Elissa Swearingen,[1] Miki Hardy,[1] Patrick Collins,[1] Bin Wu,[1] Eric Yuan,[1] Daniel Lu,[1] Chi-Ming Li,[1] Songli Wang,[1] and Michael Ollmann[1]

[1]Genome Analysis Unit, Amgen Global Research, 1120 Veteran Blvd, ASF1, South San Francisco, CA 94080, USA

Small interfering RNA (siRNA) therapeutics have developed rapidly in recent years, despite the challenges associated with delivery of large, highly charged nucleic acids. Delivery of siRNA therapeutics to the liver has been established, with conjugation of siRNA to N-acetylgalactosamine (GalNAc) providing durable gene knockdown in hepatocytes following subcutaneous injection. GalNAc binds the asialoglycoprotein receptor (ASGPR) that is highly expressed on hepatocytes and exploits this scavenger receptor to deliver siRNA across the plasma membrane by endocytosis. However, siRNA needs to access the RNA-induced silencing complex (RISC) in the cytoplasm to provide effective gene knockdown, and the entire siRNA delivery process is very inefficient, likely because of steps required for endosomal escape, intracellular trafficking, and stability of siRNA. To reveal the cellular factors limiting delivery of siRNA therapeutics, we performed a genome-wide pooled knockout screen on the basis of delivery of GalNAc-conjugated siRNA targeting the *HPRT1* gene in the human hepatocellular carcinoma line Hep3B. Our primary genome-wide pooled knockout screen identified candidate genes that when knocked out significantly enhanced siRNA efficacy in Hep3B cells. Follow-up studies indicate that knockout of *RAB18* improved the efficacy of siRNA delivered by GalNAc, cholesterol, or antibodies, but not siRNA delivered by Lipofectamine transfection, suggesting a role for *RAB18* in siRNA delivery and intracellular trafficking.

INTRODUCTION

Small interfering RNAs (siRNAs) are short (20–25 bp), double-stranded RNA molecules that operate through the RNA interference (RNAi) pathway to specifically degrade target gene mRNA.[1–5] Despite their substantial therapeutic potential, siRNA therapeutics are limited by the challenges associated with delivery of large, highly negatively charged nucleic acids into cells. Conjugation to N-acetylgalactosamine (GalNAc) has proved to be a successful strategy for hepatocyte-targeted siRNA therapeutics and has motivated research on targeted delivery of siRNA to other cell types using receptor-mediated uptake of siRNA.[6–8] On hepatocytes, GalNAc binds the highly expressed scavenger receptor ASGPR (asialoglycoprotein receptor) to deliver siRNA across the plasma membrane by clathrin-coated endosomes.[9–11] The human ASGPR exists as hetero-oligomers formed by two subunits: the major ASGR1 (asialoglycoprotein recep-

tor 1) subunit and the minor ASGR2 (asialoglycoprotein receptor 2) subunit, with ASGR1 being critical for efficient GalNAc-conjugated siRNA delivery.[12–14] Although GalNAc conjugation improves siRNA delivery, it remains an inefficient process.[15,16]

As endosomes mature, the internal pH drops and causes GalNAc-conjugated siRNAs to be released from ASGPR. The ASGPR receptors then quickly recycle back to the cell surface, while GalNAc-conjugated siRNAs remain inside the endosome.[15] Endosomal glycosidases then work to cleave GalNAc from siRNA conjugates.[15] Fewer than 1% of the remaining free siRNAs are estimated to escape from endosomes through an unknown mechanism and have access to RISC in the cytoplasm to provide effective gene knockdown.[16] After siRNA enters the cell, it remains inactive until becomes loaded into the core component of RISC. The passenger (sense) strand is removed, and the guide (antisense) strand is then bound to catalytic Argonaute 2 (Ago2).[17,18] The siRNA guide strand then guides and aligns the RISC complex on the target mRNA and induces cleavage of the target mRNA through the catalytic function of Ago2. The siRNA intracellular trafficking and escape steps are very inefficient, and the underlying mechanisms are not fully understood.[15,19]

In recent years, adaptation of the bacterial CRISPR-Cas9 system to mammalian cells have enabled genome-wide loss-of-function screens to identify new biological mechanisms.[20–24] To reveal the cellular factors limiting delivery of siRNA therapeutics, we performed a genome-wide pooled CRISPR-Cas9 screen (referred as CRISPR screen in the rest of this article) on the basis of delivery of GalNAc-conjugated siRNA targeting the *HPRT1* gene in the human hepatocellular carcinoma line Hep3B. Multiple candidate genes that when knocked out significantly enhance siRNA efficacy in Hep3B cells were identified from the CRISPR screen. A secondary arrayed CRISPR screen using multiplexed synthetic gRNA in 96/384-well format was then used to
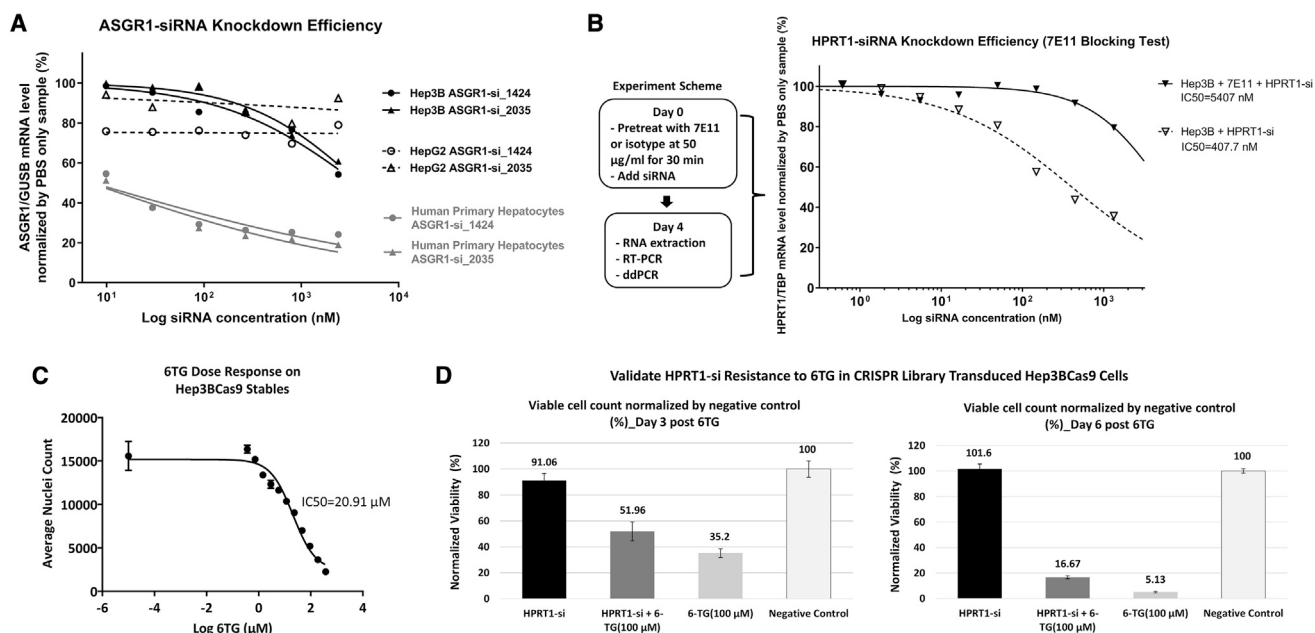
Figure 1. Validation of screen conditions for genome-wide pooled CRISPR-Cas9 screen

(A) Comparison of target gene (*ASGR1*) silencing potency in human primary hepatocytes, Hep3B and HepG2 cells by two GalNAc-conjugated *ASGR1* siRNAs. The features of these two siRNA conjugates are described in Table S2. (B) Treatment with an in-house-made anti-ASGR1 antibody, 7E11, mitigated the *HPRT1* gene silencing induced by GalNAc-*HPRT1* siRNA (8172) in Hep3B cells. The left panel outlines the experiment scheme, and the right panel shows the ddPCR measurement of *HPRT1* mRNA levels in percentage normalized by housekeeping gene *TBP* (TATA box binding protein) readings and no siRNA (PBS only) treated control group. The feature and sequence of siRNA 8172 is described in Table S2. (C) Dose-dependent kill curve of 6TG treatment in Hep3BCas9 cells. (D) A small-scale pilot experiment to validate the feasibility of using HPRT1-6TG live/dead selection for CRISPR screen. The gRNA lentivirus library transduced Hep3BCas9 cells were treated with GalNAc-*HPRT1* siRNA and/or 6TG (100 μL) in different groups. The viable cell count measured by ViCell on day 3 and day 6 after 6TG treatment for each treatment group was normalized by negative control group readings. The resulting normalized viability percentage of each group at both time points was plotted into bar graph. Left panel: day 3 post-6TG treatment data. Right panel: day 6 post-6TG treatment data. Error bars indicate SD (standard deviation) of three replicates.

validate these candidate genes. Additional follow-up studies of one top candidate gene, *RAB18*, indicate that knocking out *RAB18* improves siRNA silencing potency for siRNA delivered by conjugation to GalNAc, cholesterol, or anti-ASGR1 antibodies, but not by Lipofectamine transfection. The results of this study provide insights into mechanisms of siRNA delivery and may guide development of improved siRNA therapeutics.

RESULTS

Hep3B cells demonstrate dose-dependent knockdown of target gene through GalNAc-conjugated siRNA-induced silencing

An ideal system for identifying key regulators of GalNAc-conjugated siRNA-induced silencing would have the following attributes: (1) long-term maintenance; (2) stable Cas9 expression; (3) lentiviral transducibility; and (4) efficient RNAi response to siRNA delivered by multiple delivery methods, including GalNAc-mediated siRNA uptake. Human primary hepatocytes have been proved to internalize GalNAc-conjugated siRNA through cell surface ASGPR.[9–11] However, large-scale CRISPR screens have been challenging in human primary hepatocytes because of their limited proliferative potential. We therefore explored the possibility of using human hepatocellular carcinoma cell lines such as HepG2 or Hep3B to perform our CRISPR

screen. Although both HepG2 and Hep3B cells express high levels of *ASGR1* and *ASGR2* (Table S1), only Hep3B cells displayed dose-dependent knockdown of target gene through GalNAc-conjugated siRNA-induced silencing (Figure 1A; Table S2). The siRNA concentration required for knockdown in Hep3B cells was substantially higher than what is needed in primary human hepatocytes, but the level of silencing was sufficient for CRISPR screening, particularly for screens looking for enhancers of siRNA delivery and activity.

To further validate whether GalNAc-conjugated siRNA-induced silencing in Hep3B is mediated through ASGR1, an antibody-blocking test was performed (Figure 1B). Hep3B cells were first pre-incubated with an in-house-generated anti-ASGR1 antibody (7E11) or no antibody treatment as control for 30 min, followed by treatment with GalNAc-conjugated siRNA targeting *HPRT1* (GalNAc-*HPRT1* siRNA: 8172) (Table S2) at multiple doses. The target gene (*HPRT1*) mRNA levels were measured on day 4 after siRNA treatment using ddPCR (digital droplet polymerase chain reaction) analysis. As indicated in Figure 1B, application of the ASGR1-specific antibody reduced siRNA silencing efficacy (13-fold higher IC_{50} for anti-ASGR1 treatment [5,404 nM] relative to no antibody treatment [407.7 nM]).

After establishing the suitability of Hep3B for GalNAc-conjugated siRNA-induced silencing, we then generated Hep3B cells stably expressing Cas9. The editing capability of the Cas9-stable Hep3B was assayed by validating their editing efficacy on two target genes, *SLC3A2* and *ASGR1* (Table S3; Figure S1). The Cas9-stable Hep3B cells (referred as Hep3BCas9 in the rest of this article) were then used to perform the CRISPR screen to search for regulators of GalNAc-conjugated siRNA-induced silencing.

HPRT1-6TG (6-thioguanine) live/dead selection-based CRISPR screen in Hep3BCas9 cells

Live/dead selection provides an efficient format for pooled screens, and we chose the established HPRT1-6TG-based live/dead selection system for this CRISPR screen to identify genes that regulate the activity of siRNA delivered by GalNAc-mediated internalization. 6-Thioguanine (6TG), a purine analog, is incorporated into DNA and RNA after being phosphorylated by hypoxanthine phosphoribosyl transferase (encoded by *HPRT1*), resulting in cell death.[25] To develop our screening protocol, we designed and validated a GalNAc-conjugated siRNA targeting human *HPRT1* incorporating 2′-fluoro (F) and 2′-O-methyl (OMe) modifications commonly used in siRNA therapeutics (GalNAc-*HPRT1* siRNA: 8172; Table S2). Knockdown of *HPRT1* by the GalNAc-*HPRT1* siRNA would be expected to confer resistance to 6TG, providing a live/dead screening phenotype on the basis of the uptake and activity of GalNAc-*HPRT1* siRNA. In the context of our CRISPR screen, knockout of genes whose function restricts activity of the GalNAc-*HPRT1* siRNA would increase *HPRT1* knockdown and cell viability in the presence of 6TG. Conversely, knockout of genes required for GalNAc-*HPRT1* siRNA activity would limit *HPRT1* knockdown and reduce cell viability in the presence of 6TG. One limitation of the HPRT1-6TG screening phenotype is that many other gene knockouts can alter cell viability and sensitivity to 6TG. Distinguishing these genes from genes regulating uptake and activity of GalNAc-conjugated siRNA requires running parallel CRISPR screens with and without GalNAc-*HPRT1* siRNA or 6TG treatment.

To establish our screening protocols, we determined the 6TG kill curve in Hep3BCas9 cells (Figure 1C) and performed a small-scale pilot screen using 100 μM 6TG (∼IC70) (Figure 1D) and 20 μM 6TG (∼IC50) (Figure S2). An 80k genome-wide CRISPR gRNA lentivirus library (CRISPR KOHGW 80K [lot #17050301]; Cellecta, Mountain View, CA) was transduced into Hep3BCas9 cells to generate a genome-wide knockout pool. These gRNA-transduced cells were then analyzed for their ability to be selected using GalNAc-*HPRT1* siRNA and 6TG. As illustrated in Figure 1D, cells were divided into four groups: (1) siRNA only, (2) siRNA with 6TG treatment, (3) 6TG only, and (4) no treatment (negative control). To obtain sufficient but not excessive siRNA effect, 750 nM (about IC60) GalNAc-*HPRT1* siRNA (8172) was used. On day 3 after 6TG treatment, the 100 μM 6TG-only group had 35.2% viable cells, while the *HPRT1*-si + 100 μM 6TG group had 51.96% viable cells (Figure 1D). On day 6 after 6TG treatment, the 100 μM 6TG-only group had only 5.13% viable cells, while the *HPRT1*-si + 100 μM 6TG group had 16.67% viable cells

(Figure 1D). These results indicate that GalNAc-*HPRT1* siRNA treatment was partially protective, providing a screening phenotype well suited for detecting gene knockouts that enhance RNAi activity. On the basis of our findings from this pilot screen, we chose to use 6-day 100 μM 6TG treatment as the condition for the genome-wide CRISPR screen. To ensure that we covered an optimal siRNA dose range, the CRISPR screen was done with 150 nM GalNAc-*HPRT1* siRNA (low-dose group) and 750 nM GalNAc-*HPRT1* siRNA (high-dose group). Our CRISPR screen experimental scheme is diagrammed in Figure 2A. The genomic DNA samples were extracted from all sample pellets collected during the screen and analyzed by NGS (next-generation sequencing) barcode sequencing.

NGS sequencing results

The NGS sequencing results were analyzed by a previously described algorithm.[26] A false discovery rate (FDR) of <0.2 was used as cutoff line. To assess the quality of the screen, we examined gRNA library representation throughout the screen to detect any skewing that might bias our findings. As shown in Figures S3A and S3B, all samples maintained good representation of gRNA library: roughly 77,000 gRNAs present with similar overall distribution. The deletion efficacy of this CRISPR screen was assessed by performing essential gene depletion analysis. As demonstrated in Figure S3C, more than 78% of the cell essential genes were depleted in the baseline sample compared with the gRNA plasmid library. In addition, gRNAs that target *HPRT1* were successfully enriched by roughly 2-fold in the 6TG-treated versus no-6TG group (Figure S4). We then looked for additional genes that may play key roles in regulating GalNAc-conjugated siRNA activity.

In order to identify genes that when knocked out can improve GalNAc-conjugated siRNA internalization, trafficking, or RNAi activity, we focused on gRNAs that were enriched in samples treated with both siRNA and 6TG but were not enriched in the 6TG-only-treated control group. To select the genes with the most potent effects, we selected gene hits that were significantly (FDR < 0.2) enriched in both high-dose (750 nM) and low-dose (150 nM) GalNAc-*HPRT1* siRNA with 6TG treatment groups, compared with the 6TG-only treatment group (Figure 2B). This analysis identified 17 genes (Figure 2B) whose function potentially restricts the delivery and activity of GalNAc-siRNA. Despite our use of parallel screens to distinguish siRNA-dependent from siRNA-independent screen hits, genes that affect sensitivity to 6TG even in the absence of siRNA might be included in this set of 17 genes because of variability among screen arms. To determine whether any of these 17 genes affect 6TG sensitivity in the absence of siRNA, we plotted the genes depleted in the 6TG-only-treated group versus no-treatment group. In Figure 2C, the horizontal axis indicates the sensitivity to 6TG, and the 17 genes of interests are highlighted. With FDR < 0.2 as the cutoff, 8 of the 17 genes of interest were identified as promoting sensitivity to 6TG treatment even in the absence of any siRNA treatment (Figure 2C). The 9 remaining genes that when knocked out have no impact on 6TG sensitivity in the absence of siRNA have larger FDRs on horizontal axis, and these genes (*RAB18*, *YAP1*, *CCNE1*, *SLC30A9*, *C14orf80*, *HIF1AN*, *TRAF2*, *NAPG*, and *SCFD2*) are the most interesting to
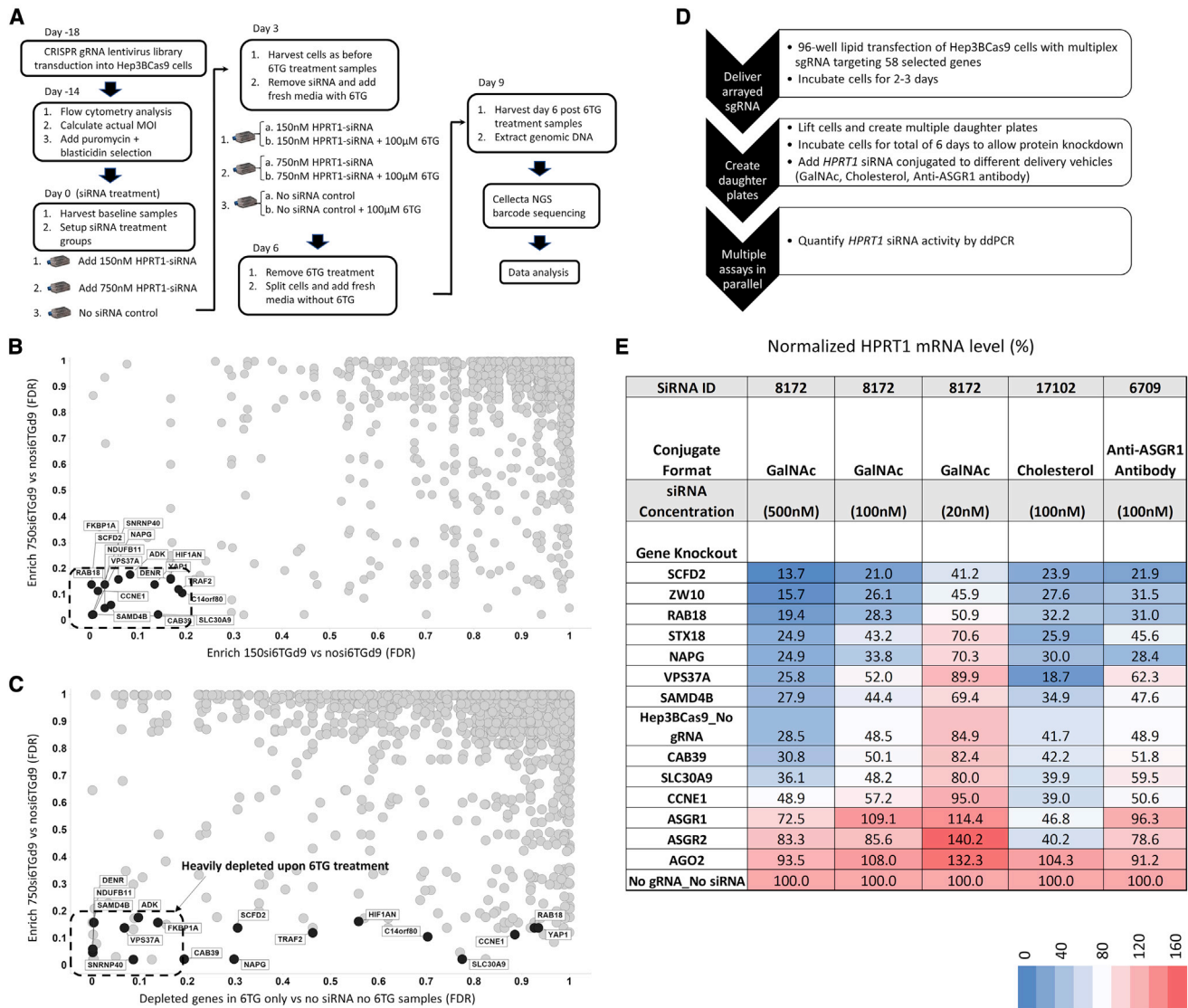
Figure 2. Large-scale genome-wide pooled CRISPR-knockout screen experiment and candidate gene validation

(A) Experiment scheme of large-scale genome-wide pooled CRISPR-knockout screen. (B) Analysis of the CRISPR screen results by overlapping enriched genes in both 150 nM siRNA + 6TG treated samples (150si6TGd9) versus no siRNA but 6TG treated samples (nosi6TGd9) and 750 nM siRNA + 6TG treated samples (750si6TGd9) versus no siRNA but 6TG treated samples (nosi6TGd9). A total of 17 genes were identified with FDR < 0.2 (outlined by dashed line). (C) Analysis of the CRISPR screen results by overlapping enriched genes from 750 nM siRNA + 6TG treated samples (750si6TGd9) versus no siRNA but 6TG treated samples (nosi6TGd9) with depleted genes in 6TG only vs no siRNA no 6TG samples. The horizontal axis indicates the sensitivity to 6TG. The dashed line outlines 8 genes with FDR < 0.2 that were heavily depleted upon 6TG treatment. (D) Experiment scheme for testing of regulators of *HPRT1* siRNA activity using secondary arrayed multiplexed synthetic gRNA screening in 96-well format. (E) Heatmap results of secondary arrayed multiplexed synthetic gRNA shown in (C). In the heatmap, red indicates reduced *HPRT1* siRNA silencing activity, and blue indicates enhanced *HPRT1* siRNA silencing activity. Colors indicate the percentage of *HPRT1/TBP* mRNA signals detected through ddPCR and normalized to no siRNA control.

us because their enrichment is more likely to be related to siRNA delivery and activity.

Validation of primary CRISPR screen hits by secondary arrayed CRISPR screen

To confirm hits from the pooled screen and move beyond the limitations of the 6TG live/dead phenotype, we characterized selected genes using arrayed gRNA and direct quantification of siRNA activity by ddPCR. We used a multiplexed synthetic gRNA system to achieve efficient knockout of target genes in 96-well format without clonal isolation. In this multi-guide strategy, three gRNAs designed in close proximity to one another are delivered together to Cas9+ cells to induce efficient target gene knockout (Figure S5).
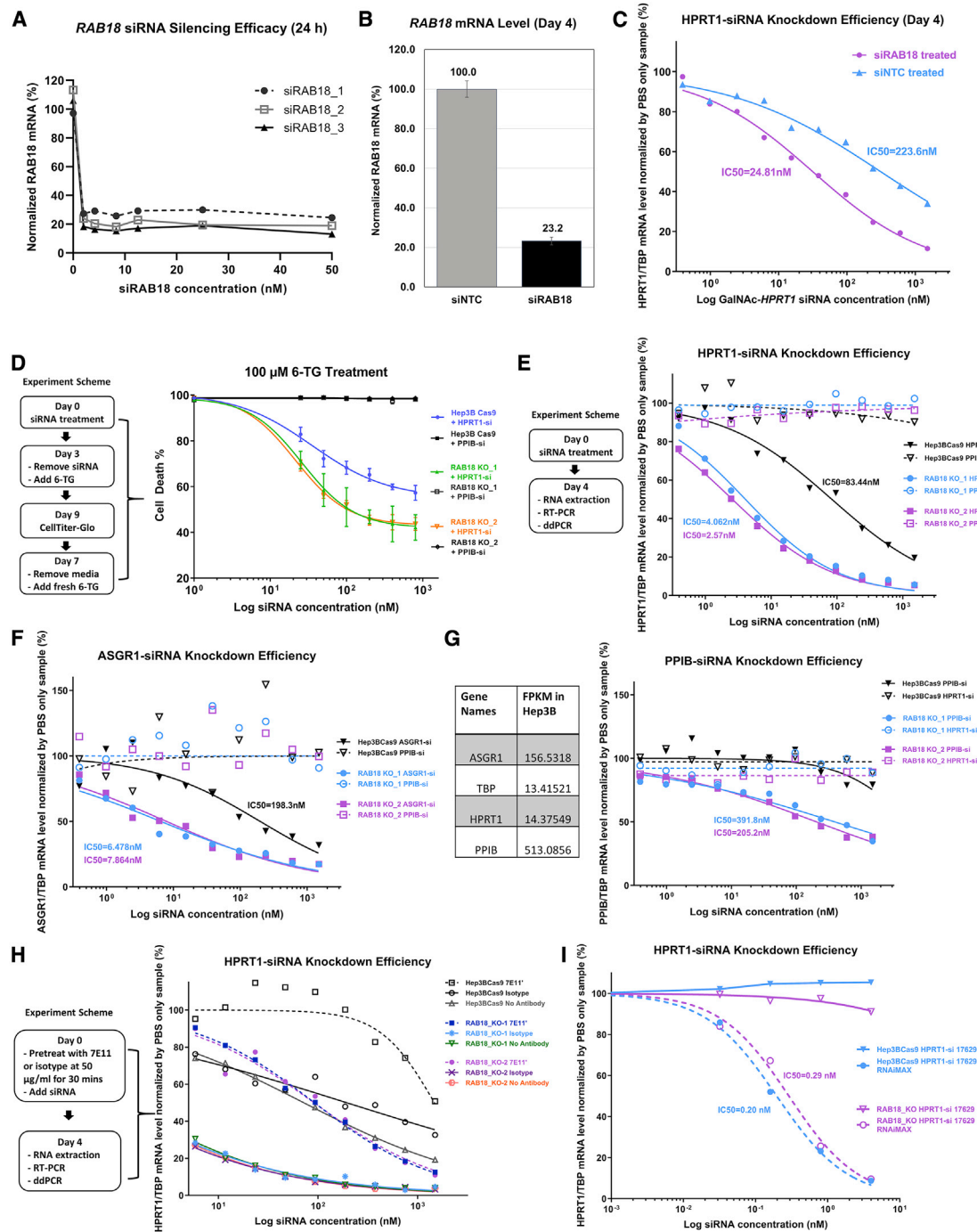
Figure 3. Validation of the effect of *RAB18* knockdown and knockout on siRNA silencing potency

(A) Twenty-four hour knockdown efficacy of three siRNA molecules targeting *RAB18* in Hep3B cells. Plotted are the ddPCR measured *RAB18* mRNA levels. (B) The ddPCR measurement of *RAB18* mRNA levels in the cells used for analysis described in (C) on day 5 after siRAB18 and siNTC treatment, or day 4 after GalNAc-*HPRT1* siRNA treatment. Error bars indicate SD of three replicates. (C) Measurement of GalNAc-*HPRT1* siRNA silencing potency in both siRAB18_3 and siNTC-treated Hep3B cells by ddPCR on day 4 after GalNAc-*HPRT1* siRNA treatment. Plotted are the ddPCR-measured *HPRT1* mRNA levels. (D) HPRT1-6TG live/dead selection performed in both Hep3BCas9 and *RAB18*-knockout cells. The left panel outlines the experiment scheme, and the right panel shows the cell death rate measured with CellTiter-Glo reagents (Promega, Madison, WI). (E) Measurement of GalNAc-*HPRT1* siRNA silencing potency in both Hep3BCas9 and *RAB18*-knockout cells by ddPCR on day 4 after siRNA treatment. The left panel summarizes the experiment scheme, and the right panel shows the ddPCR-measured *HPRT1* mRNA levels. *PPIB* siRNA was used as control siRNA. (F)

As illustrated in Figure 2D, the multiplexed synthetic gRNAs for genes identified in our initial CRISPR screen (*RAB18*, *CCNE1*, *SLC30A9*, *NAPG*, *SCFD2*, *VPS37A*, *SAMD4B*, and *CAB39*) along with some control genes (*AGO2*, *ASGR1*, and *ASGR2*) were transfected into Hep3BCas9 cells. CRISPR-knockout cells generated in this manner were then treated with GalNAc-*HPRT1* siRNA or *HPRT1* siRNA delivered through other conjugation formats (anti-ASGR1 antibody-conjugated *HPRT1* siRNA [6709] and cholesterol-conjugated *HPRT1* siRNA [17102]; Table S2). A heatmap of *HPRT1* siRNA silencing efficacy as measured using ddPCR (normalized to no-siRNA control) is shown in Figure 2E. As expected, when *AGO2* was knocked out by multiplexed synthetic gRNA, the *HPRT1* siRNA silencing activity was abolished in all tested siRNA conjugates. Because ASGR1 is a critical component of ASGPR receptor, ASGR1 knockout led to loss of response to GalNAc-*HPRT1* siRNA as well as to anti-ASGR1 antibody-conjugated *HPRT1* siRNA. However, knocking out *ASGR1* had no impact on the function of cholesterol-conjugated *HPRT1* siRNA. These results indicate that the multiplexed synthetic gRNA system was working as expected. In agreement with the pooled screening results, knockout of *RAB18*, *SCFD2*, *NAPG*, or *SAMD48* by multiplexed synthetic gRNA enhanced *HPRT1* mRNA knockdown by GalNAc-*HPRT1* siRNA and showed similar enhancement of *HPRT1* siRNA delivered by cholesterol or anti-ASGR1 antibody (Figure 2E). *VPS37A* specifically enhanced cholesterol-conjugated siRNA efficacy. Other screen hits, *CAB39*, *CCNE1*, and *SLC30A9*, were not validated by the multiplexed synthetic gRNA approach. Our arrayed gRNA library also included gRNA targeting the *ZW10* and *STX18* genes, on the basis of reports that the proteins they encode interact with RAB18 protein.[27,28] Similar to RAB18, knocking out *ZW10* and *STX18* by multiplexed synthetic gRNA enhanced siRNA silencing efficacy (Figure 2E).

RAB18 knockdown/knockout enhances the silencing effects of multiple siRNA conjugates

Because *RAB18* was the only RAB family member detected in our CRISPR screen, and because the RAB family is important in regulating intracellular vesicle trafficking, we decided to focus on understanding the mechanisms by which *RAB18* regulates siRNA activity. To study the function of *RAB18*, three *RAB18*-specific siRNA molecules (siRAB18_1, siRAB18_2, and siRAB18_3, from Ambion; Table S4) were validated for their silencing potency of *RAB18* in Hep3B cells following transfection. Among three tested siRNA molecules, siRAB18_3 showed the best knockdown of *RAB18* (Figure 3A) and was used for further studies. Hep3B cells transfected with either siRAB18_3 or a non-targeting control siRNA molecule (siNTC) for

24 h were further treated with GalNAc-*HPRT1* siRNA at various concentrations. As illustrated in Figure 3B, siRAB18_3 transfection resulted in 77% knockdown by ddPCR compared with the control siRNA-treated cells. To determine whether *RAB18* knockdown affected the efficacy of GalNAc-*HPRT1* siRNA treatment, the level of *HPRT1* mRNA was also measured by ddPCR on day 4 post GalNAc-*HPRT1* siRNA treatment. As shown in Figure 3C, the knockdown of *HPRT1* was greater in siRAB18_3-treated Hep3B cells compared with siNTC-treated Hep3B cells. The IC$_{50}$ values for siRAB18_3-treated cells and siNTC-treated cells were 24.8 versus 223.6 nM (Figure 3C), respectively, a 10-fold change.

To completely abolish the function of *RAB18*, we created two *RAB18*-knockout pools (RAB18_KO_1 and RAB18_KO_2) by transducing two lentiviral gRNA vectors targeting *RAB18* (SIGMA vector: U6-gRNA: PGK-puro-2A-tagBFP) into Hep3BCas9 cells (Figure S6A). The *RAB18*-knockout efficiency was verified using Amplicon-EZ sequencing (GENEWIZ, Newbury Park, CA) (Figures S6B and S6C). Knocking out *RAB18* did not alter cell viability (Figure S6D). Because *RAB18* was identified through the HPRT1-6TG selection screen, we first repeated the same assay in *RAB18*-knockout cells. When treated with multiple doses of GalNAc-*HPRT1* siRNA followed by 100 μM 6TG, *RAB18*-knockout cells were resistant to 6TG compared with Hep3BCas9 cells (42% cell death in *RAB18*-knockout cells compared with 57% cell death in Hep3BCas9 cells at the highest siRNA dose tested; Figure 3D), indicating that *HPRT1* siRNA induced greater gene silencing in *RAB18*-knockout cells than in Hep3BCas9 parental cells. Neither Hep3BCas9 cells nor *RAB18*-knockout cells treated with GalNAc-conjugated siRNA targeting the *PPIB* gene (8714) as a non-relevant siRNA control showed enhanced resistance to 6TG treatment (Figure 3D; Table S2). We also used ddPCR to directly measure siRNA silencing activity in *RAB18*-knockout cells. As illustrated in Figures 3E–3G, Hep3BCas9 cells and *RAB18*-knockout cells were treated with three GalNAc-conjugated siRNAs: *HPRT1* siRNA, *ASGR1* siRNA (16084) (Table S2), and *PPIB* siRNA. For all three tested siRNAs, the target gene knockdown was greater in *RAB18*-knockout cells compared with Hep3BCas9 parental cells (Figures 3E–3G). The IC$_{50}$ for *HPRT1* siRNA in Hep3BCas9 or two *RAB18*-knockout lines was 83.4 nM versus 2.6 or 4.1 nM (Figure 3E), respectively, a 20- to 30-fold change. When tested using GalNAc-*ASGR1* siRNA, the IC$_{50}$ was 198.3 nM in Hep3BCas9 cells and 7.9 or 6.5 nM in two *RAB18*-knockout cells (Figure 3F). *PPIB* is a highly expressed gene in Hep3B cells (Figure 3G) that could not be silenced by our GalNAc-*PPIB* siRNA in Hep3BCas9 cells (Figure 3G). However, the same *PPIB* siRNA was able to silence *PPIB* in two

Measurement of GalNAc-*ASGR1* siRNA silencing potency in both Hep3BCas9 and *RAB18*-knockout cells by ddPCR on day 4 post siRNA treatment. The experiment scheme is the same as shown in (E). Plotted here are *ASGR1* mRNA levels measured by ddPCR. *PPIB* siRNA was used as control siRNA. (G) The same experiment shown in (E) was performed using GalNAc-*PPIB* siRNA. The left panel lists the expression profiles of target genes in FPKM (fragments per kilobase of transcript per million mapped reads) (obtained from Broad Institute Cancer Cell Line Encyclopedia [CCLE]). The right panel plots the ddPCR measurement of *PPIB* mRNA levels. *HPRT1* siRNA was used as control siRNA. (H) Antibody-blocking test in Hep3BCas9 and *RAB18*-knockout cells by using anti-ASGR1 antibody 7E11. The left panel summarizes the experiment scheme, and the right panel shows the ddPCR measurement of *HPRT1* mRNA levels. (I) Unconjugated *HPRT1* siRNA transfection assay in Hep3BCas9 and *RAB18*-knockout cells. Plotted are the ddPCR-measured *HPRT1* mRNA levels on day 4 after siRNA treatment. All ddPCR results shown were normalized by *TBP* and no siRNA (PBS only) treated control group.

$RAB18$-knockout pools (IC_{50} = 205.2 or 391.8 nM) (Figure 3G). To investigate whether $RAB18$ knockout alters the duration of action of a GalNAc-siRNA, the siRNA silencing efficacy at a later time point (11 days after siRNA delivery) was also checked using ddPCR (Figures S7A–S7C). Although the silencing effect declined as the cells proliferated over time, the silencing potency remained greater in $RAB18$-knockout cells than in Hep3BCas9 cells. For example, when treated with GalNAc-$HPRT1$, the IC_{50} at day 11 was 363.6 nM in Hep3BCas9 cells and 41.3 or 58.3 nM in two $RAB18$-knockout pools (Figure S7A). These results lead us to conclude that $RAB18$ knockout enhances the silencing potency of GalNAc-conjugated siRNA as well as cholesterol and antibody-conjugated siRNA.

Gene silencing induced by GalNAc-conjugated siRNA in *RAB18*-knockout cells requires ASGR1

As discussed and tested earlier, GalNAc-siRNA conjugate-induced gene silencing is mediated through ASGR1. We therefore tested if ASGR1 was required for GalNAc-siRNA conjugates to function in $RAB18$-knockout cells using an antibody-blocking test (Figures 3H, S7D, and S7E). As shown in Figure 3H, the application of 7E11 was able to reduce the siRNA silencing efficacy of $HPRT1$ gene in Hep3BCas9 and $RAB18$-knockout cells. Similar results were obtained when the same experiment was performed using $ASGR1$ siRNA and $PPIB$ siRNA to silence $ASGR1$ and $PPIB$ (Figures S7D and S7E). Like what we observed in Hep3B cells, the GalNAc-siRNA conjugates rely on ASGR1 to enter $RAB18$-knockout cells. The two individually generated $RAB18$-knockout pools behaved identically in all tests. Therefore, only one $RAB18$-knockout pool was used for the rest of the related experiments (referred as RAB18_KO). To investigate whether knocking out $RAB18$ enhances siRNA silencing efficacy by improving siRNA internalization, a flow cytometry-based siRNA internalization assay was performed by delivering AF647-labeled GalNAc-conjugated $HPRT1$ siRNA to Hep3BCas9 and RAB18_KO cells. As illustrated in Figure S8, RAB18_KO cells exhibited similar siRNA internalization rate compared with Hep3BCas9 cells in the tested experimental duration, indicating that the enhanced siRNA silencing efficacy observed in RAB18_KO cells was not caused by increasing siRNA uptake.

RAB18 knockout has no impact on the activity of siRNA delivered through lipofectamine transfection

Lipofectamine transfection-mediated siRNA delivery induces mRNA knockdown at low siRNA concentrations, likely because of the ability of Lipofectamine to help siRNA circumvent some of the intracellular barriers encountered by alternative delivery methods such as GalNAc, cholesterol, and antibody-mediated uptake.[29] After confirming that knocking out $RAB18$ enhances siRNA potency delivered through GalNAc conjugates, we asked if knocking out $RAB18$ could enhance siRNA potency delivered by Lipofectamine-mediated transfection. To address this question, we used an unconjugated $HPRT1$ siRNA (17629) (Table S2) to treat Hep3BCas9 and RAB18_KO cells at various concentrations with or without Lipofectamine RNAiMAX reagent (Invitrogen, Waltham, MA). As summarized in Figure 3I, the

activity of siRNA delivered by Lipofectamine was not altered by $RAB18$ knockout. Lipofectamine reagents efficiently silenced the target gene $HPRT1$ with nearly identical IC_{50} values in Hep3BCas9 (IC_{50} = 0.2 nM) and RAB18_KO cells (IC_{50} = 0.3 nM).

DISCUSSION

The HPRT1-6TG selection-based CRISPR-Cas9 screen performed in Hep3B background has successfully identified several key regulators of GalNAc-conjugated siRNA activity. Some of the hits from this screen, such as $RAB18$, $SCFD2$, $NAPG$, and $VPS37A$, have been validated through a secondary arrayed CRISPR screen system by using multiplexed synthetic gRNA. Here, we focused our efforts on studying the effects of $RAB18$ on siRNA delivery and activity.

Having confirmed that knocking out $RAB18$ enhances siRNA silencing potency on multiple tested target genes ($HPRT1$, $ASGR1$, and $PPIB$) and through multiple siRNA delivery methods (GalNAc, cholesterol, and antibody conjugates), we attempted to elucidate the linkage between $RAB18$ function and siRNA activity. To understand whether knocking out $RAB18$ enhances siRNA silencing efficacy through improved siRNA internalization, we performed a siRNA internalization study by using AF647-labeled GalNAc-conjugated $HPRT1$ siRNA. However, knocking out $RAB18$ has no impact on the internalization of the fluorescent-labeled siRNA (Figure S8). RAB GTPases constitute the largest family of small GTPases that have important roles in regulating membrane trafficking by switching between GTP-bound "on" and GDP-bound "off" forms. There are more than 60 RAB family members in humans that are localized to distinct intracellular membranes and play important roles in regulating intracellular vesicle budding, uncoating, motility, and fusion. Once internalized, siRNA has been shown to traffic through the endocytic pathway.[30,31] We therefore expected multiple members of the RAB family to be identified in our CRISPR screen as regulators of siRNA activity, but $RAB18$ was the only RAB family member that came out of our screen (FDR < 0.2). We then reassessed the NGS data to look for other RAB family members. However, no other RAB family member was significantly enriched in the live cell population. This could be due to the limitations of this screen. First, the live/dead selection represents a very harsh cutoff for improving siRNA silencing potency. Second, the CRISPR-Cas9 screen described here is designed to identify genes whose loss enhances siRNA silencing efficacy. Therefore, RAB family members whose functions are required for siRNA activity could be dropped off from this screen. Finally, siRNA-induced gene silencing is a complex process, in which multiple genes may be required to regulate individual steps. Therefore, one gRNA per cell strategy could miss the redundant genes, such as RAB family members.

As one of the 20 most highly conserved RAB GTPases present in the last eukaryotic common ancestor of both the plant and animal kingdoms,[32,33] RAB18 has diverse functions that could account for the impact of $RAB18$ knockout on siRNA delivery and activity. Studies have linked $RAB18$ to regulation of lipid droplet (LD) formation,[27,34]

inhibition of COPI-independent retrograde trafficking from Golgi to endoplasmic reticulum (ER),[35] regulation of secretory granules[36] and peroxisomes,[37] promotion of hepatitis C virus (HCV) assembly on the LD membrane,[38] and regulation of ER structure.[39] It is very difficult to tease out which known functions of *RAB18* gene might contribute to regulation of siRNA activity or whether a novel function of *RAB18* needs to be identified. However, several lines of evidence may provide a clue to a potential mechanism by which *RAB18* influences siRNA delivery and activity. First, the NRZ (NAG-RINT1-ZW10) tethering factors and their associated ER-localized SNAREs (Use1, Syntaxin18, and BNIP1) form a complex with GTP-bound form of RAB18 protein to mediate ER-LD contact formation.[27,28] Similar to *RAB18*, knocking out *ZW10* and *STX18* (encoding Syntaxin18) by multiplexed synthetic gRNA enhanced siRNA silencing efficacy (Figure 2E), suggesting that ER-LD tethering regulates siRNA trafficking and activity. The siRNA-mediated degradation of target mRNA has been shown to take place in the cytoplasm.[40] However, the subcellular sites of RNA silencing remain under debate. Intriguingly, ER as a site for protein translation mediated by ribosomes has been shown to be a central nucleation site of siRNA-mediated RNA silencing.[41] In addition, an ER membrane resident protein CLIMP-63 has been proved to interact with and stabilize Dicer.[42] As indicated in these studies, ER might serve as a subcellular silencing site for siRNA. After being internalized into endosomes, the siRNA inside endosomes could travel to ER through retrograde transport. There are two different pathways of retrograde transport: the COPI-dependent and the COPI-independent pathways. Interestingly, *RAB18* loss of function mutants had been shown to specifically enhance COPI-independent retrograde Golgi-ER transport.[35] Although the exact molecular mechanisms by which *RAB18* regulates siRNA activity are not clear, the substantial improvement in siRNA activity observed in *RAB18*-knockout cells (>20-fold reduction in IC_{50} values) supports that further studies in this area could guide the development of siRNA therapeutics. Our finding that *RAB18* affects the activity of siRNA delivered by GalNAc, cholesterol, or antibodies, but not Lipofectamine transfection, highlights the relevance of *RAB18* in the development of novel siRNA delivery methods to hepatocytes and other cell types. *RAB18* is a universally expressed gene across multiple tissue types and is highly conserved across species. It would therefore be interesting to see if *RAB18* knockout in other cell or tissue types can also enhance siRNA activity.

Despite the success of our HPRT1-6TG selection screen in identifying candidate regulators of siRNA activity, there were some limitations to this approach. Our data indicate that live/dead selection using *HPRT1* siRNA and 6TG selection is not a highly sensitive way to detect changes in siRNA activity, likely because residual *HPRT1* activity after RNAi confers some resistance to 6TG. Our follow-up study using ddPCR to directly measure knockdown of *HPRT1* mRNA showed that by knocking out *RAB18*, the siRNA IC_{50} dose of *HPRT1* siRNA could be reduced by 20- to 30-fold (Figure 3E), indicating that *RAB18* is a strong regulator of siRNA activity. However, when both Hep3BCas9 and *RAB18*-knockout cells were challenged with *HPRT1* siRNA and 6TG selection, the cell survival rate was only

changed from 43% in Hep3BCas9 cells to 58% in *RAB18*-knockout cells at the highest siRNA dose tested (Figure 3D). This suggests that only gene knockouts that substantially improve *HPRT1* siRNA activity would be detected by the 6TG selection scheme. In addition, the partial knockdown of *HPRT1* in Hep3B at the screening doses of GalNAc-*HPRT1* siRNA provided limited resistance to 6TG, making the screen more suitable for detecting strong enhancers of RNAi rather than suppressors.

We report here the identification, using a genome-wide pooled CRISPR-Cas9 screen, of a single gene (*RAB18*) that, when knocked out, can enhance siRNA-mediated gene silencing by at least 20-fold (IC_{50}) in Hep3B cells. Given the current interest in using siRNA as a therapeutic modality and the need for improved delivery methods, identification of this key regulator may allow the development of future pharmacological strategies to enhance siRNA efficacy.

MATERIALS AND METHODS
Cell line and culture condition
The Hep3B cells were purchased from ATCC (Manassas, VA). The culture condition for Hep3B cells is as follows: EMEM (Eagle's minimum essential medium; catalog #30-2003; ATCC) + 10% FBS (fetal bovine serum). The culture condition for Hep3Bcas9 cells is as follows: EMEM +10% FBS + 10 µg/mL blasticidin. The culture condition for *RAB18*-knockout cells is as follows: EMEM + 10% FBS + 10 µg/mL blasticidin + 0.5 µg/mL puromycin.

Generation of Hep3BCas9 cells and validation of their editing function
A TransEDIT CRISPR Cas9 nuclease expression lentivirus (pCLIP-Cas9-Nuclease-EFS-Blast) ordered from TransOMIC technologies (catalog #NC0956087; Huntsville, AL) was transduced at several multiplicities of infection (MOIs) (0.5, 1, and 2) into Hep3B cells to generate Cas9-stable pools: Hep3BCas9_0.5, Hep3BCas9_1, and Hep3BCas9_2, respectively. All cells were selected and maintained with 10 µg/mL blasticidin after transduction. No toxicities were observed in all Cas9-stable expression Hep3B pools. Two gRNA lentivirus vectors targeting *SLC3A2* and *ASGR1* ordered from Millipore Sigma (Table S3) were transduced individually into both the parental Hep3B cell line and each of the Cas9-stable Hep3B pools. *SLC3A2* and *ASGR1* expression levels before and after gRNA lentivirus transduction were measured by antibody staining followed by flow cytometry analysis. Compared with the parental Hep3B cell line, both target genes were successfully knocked out in all Cas9-stable Hep3B pools (Figure S1), demonstrating the Cas9-stable Hep3BCas9 cells were fully equipped with editing function. As the editing effects were similar in all three Cas9-stable Hep3B pools, the one with lowest MOI (0.5, referred as Hep3BCas9 in the rest of this article) was chosen to perform the CRISPR screen to search for key regulators of GalNAc-conjugated siRNA-induced silencing to minimized potential Cas9 toxicity.

HPRT1-6TG selection test
The feasibility of using HPRT1-6TG live/dead selection for CRISPR screen was tested in a small-scale pilot run using 100 µM 6TG (a

dose close to IC$_{70}$; Figure 1D) and 20 μM 6TG (a dose close to IC$_{50}$; Figure S2). The cells were first equally divided into four groups (0.6E+06 cells/group): (1) siRNA only, (2) siRNA with 6TG treatment, (3) 6TG only, and (4) no treatment (negative control). To obtain sufficient but not excessive siRNA effect, a 750 nM (about IC$_{60}$) GalNAc-*HPRT1* siRNA (8172) was added to groups 1 and 2 on day 0 of the experiment. On day 3 of the experiment, the tissue culture media was removed from each group, and then 100 μM 6TG (or 20 μM 6TG) was added to groups 2 and 3, while non-selection full-growth media was added to groups 1 and 4. The cells were incubated for 3 days after 6TG treatment. Then cells were then split, and the 6TG media was replaced with full-growth media without 6TG and cultured for an additional 3 days. The cell count readings (measured by ViCell) were recorded on day 3 after 6TG treatment and day 6 after 6TG treatment and plotted in Figures 1D and S2.

Large-scale genome-wide pooled CRISPR screen

An 80k genome-wide CRISPR gRNA lentivirus library (CRISPR KOHGW 80K [lot #17050301]) was purchased from Cellecta to generate a gene-knockout pool. The CRISPR KOHGW 80K library is constructed in Cellecta's pRSG16-U6-sg-UbiC-TagRFP-2A-Puro lentiviral vector that expresses gRNA under a wild-type U6 promoter and TagRFP and Puro resistance genes under a human ubiquitin C promoter. This library covers approximately 19,000 genes with 4 gRNAs for each gene. The procedure of large-scale CRISPR screen is illustrated in Figure 2A. Briefly, the gRNA lentivirus library was transduced into 9.2E+07 Hep3BCas9 cells. The actual library transduction efficiency as reflected by RFP-positive cell population (61%) was checked using flow cytometry analysis on day 4 post-transduction. On the basis of calculations, the actual gRNA lentivirus library transduction MOI was about 0.9, and the actual coverage was 1,035. The transduced cells were then selected with puromycin and blasticidin for 14 days. On day 14 post-selection, 87% of the cells were RFP positive (indicating that 87% of the cells had integrated gRNAs) on flow cytometry. On day 14 post-selection, 1E+08 cells were collected and frozen as a baseline sample. The rest of the cells were equally divided into three groups (2.4E+08 cells/group): group 1 was treated with 150 nM GalNAc-*HPRT1* siRNA as a low-dose group, group 2 was treated with 750 nM GalNAc-*HPRT1* siRNA as a high-dose group, and group 3 was set as no siRNA control. On day 3 after siRNA treatment, 2E+08 cells were collected and frozen from each group as before 6TG treatment samples, then the rest of the cells in each group were further divided into two subgroups: (1) no 6TG treatment and (2) 6TG treatment. The cell culture medium with siRNA was removed from each flask, fresh medium containing 100 μM 6TG was added into each flask of 6TG groups, and fresh medium without 6TG was added to each flask in the no 6TG treatment group. All cells were incubated for another 3 days, and all cells were then split into fresh medium without 6TG. After a final 3 day incubation, all cells were harvested. The genomic DNA samples were extracted from all samples collected by using Gentra Puregene Cell Kit (catalog #158767; Qiagen) following the user manual and sent to Cellecta for NGS barcode sequencing.

Secondary arrayed CRISPR screen

The multiplexed synthesized gRNA of each target gene for secondary arrayed CRISPR screen was designed and synthesized by Synthego Corporation (Palo Alto, CA). All gRNAs were transfected into Hep3BCas9 cells in 96-well plate format using Lipofectamine CRISPRMAX Cas9 Transfection Reagent (catalog #CMAX00008; Invitrogen). Multiplexed synthesized gRNA (1.5 μL, 0.3 μM) was first mixed with 8.5 μL Opti-MEM medium in each well. CRISPRMAX reagent (0.2 μL) diluted in 5 μL Opti-MEM medium was then added to each well and incubated at room temperature for 5–10 min. After incubation, 85 μL (15,000 cells per well) Hep3BCas9 cells were added to each well. The plate was allowed to sit for 20 min prior to placing it in 37°C tissue culture incubator, and transfection medium was replaced with EMEM containing 10% FBS and 1% AA (antibiotic antimycotic solution) at ~6 h after transfection. The cells were split in a 1:6 ratio on day 3 post-incubation. The cells were incubated for a total of 6 days after CRISPRMAX transfection to allow protein knockdown. On day 6 post-transfection, *HPRT1* siRNA conjugated to different delivery vehicles (GalNAc, cholesterol, anti-ASGR1 antibody) was added to each well at the desired concentrations (500, 100, and 20 nM) followed by a 4-day incubation period in a 37°C tissue culture incubator. The total RNA of each sample was extracted by using KingFisher Flex System (Thermo Fisher Scientific) and MagMAX mirVana Total RNA Isolation Kit (catalog #A27828; Applied Biosystems) as per manufacturer instructions. The cDNA was then synthesized from total RNA sample using the Applied Biosystems High Capacity Reverse Transcription Kit (catalog #4368813) and used to quantify siRNA activity by ddPCR.

Droplet digital polymerase chain reaction

The ddPCR reactions were assembled using Bio-Rad's ddPCR Supermix for Probes (catalog #1863010) as per manufacturer instructions. Droplets were then generated by QX200 Automated Droplet Generator (catalog #1864101; Bio-Rad). Thermal cycling reactions were then performed on C1000 Touch Thermal Cycler with 96-Deep Well Reaction Module (catalog #1851197; Bio-Rad). The reactions were then read by QX200 Droplet Reader (catalog #1864003; Bio-Rad) and analyzed using Bio-Rad's QuantaSoft software package. The predesigned primer/probe for ddPCR assays were obtained from Integrated DNA Technologies (Coralville, IA) with 3.6:1 primer-to-probe ratio. The assay ID of primer/probe used for quantifying *HPRT1* gene is Hs.PT.39a.22214821. The assay ID of primer/probe used for quantifying *ASGR1* gene is Hs.PT.56a.24725395. The assay ID of primer/probe used for quantifying *PPIB* gene is Hs.PT.58.40006718. The assay ID of primer/probe used for quantifying housekeeping gene *TBP* is Hs.PT.58.19489510. The ddPCR copy number readings (copies/20 μL) of both target gene (*HPRT1*, *ASGR1*, or *PPIB*) and housekeeping gene *TBP* were recorded for each well. The normalized target gene mRNA level was calculated by dividing the ddPCR reading of the target gene by the ddPCR reading of *TBP* taken from the same well. The resulting number of siRNA-treated sample was further divided by the number of no-siRNA-treatment sample to obtain the percentage reading of the

target gene mRNA level, which is plotted in Figures 1A–1B, 3A, 3C, 3E–3I, and S7.

siRAB18 and siNTC transfection
The siRNA molecules targeting *RAB18* gene, siRAB18_1 (Ambion Silencer Select, catalog #4390824, ID #s22703), siRAB18_2 (ID #s22704), and siRAB18_3 (ID #s22705) were purchased from Ambion (Austin, TX). The non-targeting control siRNA (siNTC; catalog #4390843) were purchased from Invitrogen. The sequence details of siRNA-targeting *RAB18* are described in Table S4. To test siRAB18 efficacy, several concentrations of each siRAB18 molecule (2–50 nM) or sterile water (negative control) was individually reverse transfected in duplicate into Hep3B cells using Lipofectamine RNAiMAX (catalog #13778075; Invitrogen). Twenty-four hours post-transfection, cells were lysed and harvested for RNA using MagMAX mirVana Total RNA Isolation kit (catalog #A27828; Applied Biosystems) and reverse transcribed for ddPCR analysis using the Applied Biosystems High Capacity Reverse Transcription Kit (catalog #4368813), according to manufacturer instructions. For analysis of the effect of *RAB18* knockdown on GalNAc-*HPRT1* siRNA efficacy in Figures 3B and 3C, siNTC (50 nM) or siRAB18-3 (50 nM) was reverse transfected into Hep3B cells. Twenty-four hours post-transfection, cells were trypsinized and washed twice in EMEM to remove residual transfection reagent, then plated into 96-well plates containing either PBS or multiple concentrations of GalNAc-*HPRT1* siRNA. On day 4 after GalNAc-*HPRT1* siRNA treatment, the cells were lysed for RNA isolation and cDNA synthesis as described above. The *HPRT1* cDNA level was then quantified using the QIAcuity digital PCR system (Qiagen).

Anti-ASGR1 antibody-blocking test
The Hep3BCas9 cells and *RAB18*-knockout cells were first pre-incubated with in-house-generated anti-ASGR1 antibody (7E11), isotype control antibody, or no antibody for 30 min, followed by adding GalNAc-*HPRT1* siRNA treatment at different doses. The final antibody concentration was 50 μg/mL, and 2,000 cells were seeded in each well. After incubating in 37°C tissue culture incubator for 4 days, the target gene (*HPRT1*) mRNA levels were measured using ddPCR analysis.

AF647-labeled GalNAc-conjugated *HPRT1* siRNA internalization assay
Hep3BCas9 and RAB18_KO cells were detached by 5 mM EDTA diluted in DPBS (pH 8) without Mg^{2+} or Ca^{2+}. Cell suspension at 2.5E+06 cells/mL concentration was then made by using Ca^{2+} Mg^{2+} free PBS buffer containing 2% FBS (buffer 1) for each cell type. Cell suspension (100 μL) was then distributed to a U-bottom 96-well plate (catalog #353077; Falcon) and incubated on ice for 10 min. Cells were spun at $300 \times g$ for 7 min at 4°C. The supernatant was aspirated and 100 μL of either ice-cold AF647-labeled GalNAc-conjugated *HPRT1* siRNA prepared in PBS with Ca^{2+} Mg^{2+} and 2% FBS (buffer 2) and 1:1,000 dilution of Invitrogen LIVE/DEAD Fixable Green Dead Cell Stain (catalog #L34970) (siRNA treated) or buffer 2 containing only LIVE/DEAD Fixable Green Dead Cell Stain (no siRNA control) was added to each well. The final concentration of siRNA in each

well was 1.5 μM. Cells were incubated on ice for 20 min to allow GalNAc-conjugated siRNA to bind with receptor, then washed twice with 200 μL ice-cold buffer 2. The cells were then resuspended in 100 μL warm cell culture media and placed at 37°C tissue culture incubator for 30 min, 2 h, 4 h, or 20 h to activate siRNA internalization. At the end of each time point, cells were dissociated using 0.05% trypsin, then spun at $300 \times g$ for 7 min at 4°C and supernatant aspirated. Ice-cold buffer 2 (100 μL) was added to each well and incubated on ice for 2 min. Cells were spun at $300 \times g$ for 7 min at 4°C. The cells were then resuspended in 100 μL ice-cold acid wash buffer made with 25 mM acetic acid in 0.5M NaCl followed by 20 min incubation on ice with mixing by pipetting every 5 min. After two washes with 200 μL ice-cold buffer 1, the cells were then fixed in 100 μL of 1% PFA in DPBS for 10 min. Cells were washed once with Ca^{2+} Mg^{2+} free PBS buffer containing 2% FBS and 2 mM EDTA (FACS buffer). The cells were then resuspended in 100 μL FACS buffer and used for flow cytometry analysis.

AUTHOR CONTRIBUTIONS
M.O., J.L., P.C., C.-M.L., and S.W. conceived and designed the study. J.L. carried out the genome-wide pooled CRISPR screen, ddPCR analysis, and *RAB18*-knockout study and drafted the manuscript. E.S. carried out initial siRNA efficacy test and 6TG sensitivity test in Hep3B cells. M.H. conducted the secondary arrayed CRISPR screen. P.C. performed the statistical analysis of NGS results. B.W. conjugated siRNA molecules tested in this study. E.Y. performed the *RAB18*-knockdown study and AF647-labled GalNAc-conjugated *HPRT1* siRNA internalization assay. D.L. carried out Amplicon_Seq analysis to assess the editing efficacy of secondary arrayed CRISPR platform. All authors contributed to manuscript revisions. All authors approved the final version of the manuscript and agree to be held at countable for the content therein.

REFERENCES
1. Chu, C.Y., and Rana, T.M. (2007). Small RNAs: regulators and guardians of the genome. J. Cell. Physiol. *213*, 412–419. https://doi.org/10.1002/jcp.21230.

2. Dowdy, S.F. (2017). Overcoming cellular barriers for RNA therapeutics. Nat. Biotechnol. 35, 222–229. https://doi.org/10.1038/nbt.3802.

3. Juliano, R.L. (2016). The delivery of therapeutic oligonucleotides. Nucleic Acids Res. 44, 6518–6548. https://doi.org/10.1093/nar/gkw236.

4. Khvorova, A., and Watts, J.K. (2017). The chemical evolution of oligonucleotide therapies of clinical utility. Nat. Biotechnol. 35, 238–248. https://doi.org/10.1038/nbt.3765.

5. Nair, J.K., Attarwala, H., Sehgal, A., Wang, Q., Aluri, K., Zhang, X., Gao, M., Liu, J., Indrakanti, R., Schofield, S., et al. (2017). Impact of enhanced metabolic stability on pharmacokinetics and pharmacodynamics of GalNAc-siRNA conjugates. Nucleic Acids Res. 45, 10969–10977. https://doi.org/10.1093/nar/gkx818.

6. Nair, J.K., Willoughby, J.L., Chan, A., Charisse, K., Alam, M.R., Qang, Q., Hoekstra, M., Kandasamy, P., Kel'in, A.V., Milstein, S., et al. (2014). Multivalent N-acetylgalactosamine-conjugated siRNA localizes in hepatocytes and elicits robust RNAi-mediated gene silencing. J. Am. Chem. Soc. 136, 16958–16961. https://doi.org/10.1021/ja505986a.

7. Chan, A., Liebow, A., Yasuda, M., Gan, L., Racie, T., Maier, M., Kuchimanchi, S., Foster, D., Milstein, S., Charisse, K., et al. (2015). Preclinical development of a subcutaneous ALAS1 RNAi therapeutic for treatment of hepatic porphyrias using circulating RNA quantification. Mol. Ther. Nucleic Acids 4, e263. https://doi.org/10.1038/mtna.2015.36.

8. Pasi, K.J., Rangarajan, S., Georgiev, P., Mant, T., Creagh, M.D., Lissitchkov, T., Bevan, D., Austin, S., Hay, C.R., Hegemann, I., et al. (2017). Targeting of antithrombin in hemophilia A or B with RNAi therapy. N. Engl. J. Med. 377, 819–828. https://doi.org/10.1056/NEJMoa1616569.

9. Baenziger, J.U., and Fiete, D. (1980). Galactose and N-acetylgalactosamine-specific endocytosis of glycopeptides by isolated rat hepatocytes. Cell 22, 611–620. https://doi.org/10.1016/0092-8674(80)90371-2.

10. Meier, M., Bider, M.D., Malashkevich, V.N., Spiess, M., and Burkhard, P. (2000). Crystal structure of the carbohydrate recognition domain of the H1 subunit of the asialoglycoprotein receptor. J. Mol. Biol. 300, 857–865. https://doi.org/10.1006/jmbi.2000.3853.

11. Pricer, W.E., Jr., and Ashwell, G. (1971). The binding of desialylated glycoproteins by plasma membranes of rat liver. J. Biol. Chem. 246, 4825–4833.

12. Spiess, M., and Lodish, H.F. (1986). An internal signal sequence: the asialoglycoprotein receptor membrane anchor. Cell 44, 177–185. https://doi.org/10.1016/0092-8674(86)90496-4.

13. Braun, J.R., Willnow, T.E., Ishibashi, S., Ashwell, G., and Herz, J. (1996). The major subunit of the asialoglycoprotein receptor is expressed on the hepatocellular surface in mice lacking the minor receptor subunit. J. Biol. Chem. 271, 21160–21166. https://doi.org/10.1074/jbc.271.35.21160.

14. Drickamer, K., Mamon, J.F., Binns, G., and Leung, J.O. (1984). Primary structure of the rat liver asialoglycoprotein receptor. Structural evidence for multiple polypeptide species. J. Biol. Chem. 259, 770–778.

15. Prakash, T.P., Graham, M.J., Yu, J., Carty, R., Low, A., Chappell, A., Schmidt, K., Zhao, C., Aghajan, M., Murray, H.F., et al. (2014). Targeted delivery of antisense oligonucleotides to hepatocytes using triantennary N-acetyl galactosamine improves potency 10-fold in mice. Nucleic Acids Res. 42, 8796–8807. https://doi.org/10.1093/nar/gku531.

16. Gilleron, J., Querbes, W., Zeigerer, A., Borodovsky, A., Marsico, G., Schubert, U., Manygoats, K., Seifert, S., Andree, C., Stoter, M., et al. (2013). Image-based analysis of lipid nanoparticle-mediated siRNA delivery, intracellular trafficking and endosomal escape. Nat. Biotechnol. 31, 638–646. https://doi.org/10.1038/nbt.2612.

17. Leuschner, P.J., Ameres, S.L., Kueng, S., and Martinez, J. (2006). Cleavage of the siRNA passenger strand during RISC assembly in human cells. EMBO Rep. 7, 314–320. https://doi.org/10.1038/sj.embor.7400637.

18. Nakanishi, K. (2016). Anatomy of RISC: how do small RNAs and chaperones activate Argonaute proteins? Wiley Interdiscip. Rev. RNA 7, 637–660. https://doi.org/10.1002/wrna.1356.

19. Springer, A.D., and Dowdy, S.F. (2018). GalNAc-siRNA conjugates: leading the way for delivery of RNAi therapeutics. Nucleic Acid Ther. 28, 109–118. https://doi.org/10.1089/nat.2018.0736.

20. Cho, S.W., Kim, S., Kim, J.M., and Kim, J.S. (2013). Targeted genome engineering in human cells with the Cas9 RNA-guided endonuclease. Nat. Biotechnol. 31, 230–232. https://doi.org/10.1038/nbt.2507.

21. Cong, L., Ran, F.A., Cox, D., Lin, S., Barretto, R., Habib, N., Hsu, P.D., Wu, X., Jiang, W., Marraffini, L.A., et al. (2013). Multiplex genome engineering using CRISPR/Cas systems. Science 339, 819–823. https://doi.org/10.1126/science.1231143.

22. Jinek, M., Chylinski, K., Fonfara, I., Hauer, M., Doudna, J.A., and Charpentier, E. (2012). A programmable dual-RNA-guided DNA endonuclease in adaptive bacterial immunity. Science 337, 816–821. https://doi.org/10.1126/science.1225829.

23. Wang, T., Wei, J.J., Sabatini, D.M., and Lander, E.S. (2014). Genetic screens in human cells using the CRISPR-Cas9 system. Science 343, 80–84. https://doi.org/10.1126/science.1246981.

24. Shalem, O., Sanjana, N.E., Hartenian, E., Shi, X., Scott, D.A., Mikkelson, T., Heckl, D., Ebert, B.L., Root, D.E., Doench, J.G., et al. (2014). Genome-scale CRISPR-Cas9 knockout screening in human cells. Science 343, 84–87. https://doi.org/10.1126/science.1247005.

25. Liao, S., Tammaro, M., and Yan, H. (2015). Enriching CRISPR-Cas9 targeted cells by co-targeting the HPRT gene. Nucleic Acids Res. 43, e134. https://doi.org/10.1093/nar/gkv675.

26. Meisen, W.H., Nejad, Z.B., Hardy, M., Zhao, H., Oliverio, O., Wang, S., Hale, C., Ollmann, M.M., and Collins, P.J. (2020). Pooled screens identify GPR108 and TM9SF2 as host cell factors critical for AAV transduction. Mol. Ther. Methods Clin. Dev. 17, 601–611. https://doi.org/10.1016/j.omtm.2020.03.012.

27. Xu, D., Li, Y., Wu, L., Li, Y., Zhao, D., Yu, J., Huang, T., Ferguson, C., Parton, R.G., Yang, H., et al. (2018). Rab18 promotes lipid droplet (LD) growth by tethering the ER to LDs through SNARE and NRZ interactions. J. Cell Biol. 217, 975–995. https://doi.org/10.1083/jcb.201704184.

28. Li, D., Zhao, Y.G., Li, D., Zhao, H., Huang, J., Miao, G., Feng, D., Liu, P., Li, D., and Zhang, H. (2019). The ER-localized protein DFCP1 modulates ER-lipid droplet contact formation. Cell Rep. 27, 343–358.e5. https://doi.org/10.1016/j.celrep.2019.03.025.

29. Cardarelli, F., Digiacomo, L., Marchini, C., Amici, A., Salomone, F., Fiume, G., Rossetta, A., Gratton, E., Pozzi, D., and Caracciolo, G. (2016). The intracellular trafficking mechanism of Lipofectamine-based transfection reagents and its implication for gene delivery. Sci. Rep. 6, 25879. https://doi.org/10.1038/srep25879.

30. Pereira-Leal, J.B., and Seabra, M.C. (2001). Evolution of the Rab family of small GTP-binding proteins. J. Mol. Biol. 313, 889–901. https://doi.org/10.1006/jmbi.2001.5072.

31. Stenmark, H., and Olkkonen, V.M. (2001). The Rab GTPase family. Genome Biol. 2. REVIEWS3007. https://doi.org/10.1186/gb-2001-2-5-reviews3007.

32. Elias, M., Brighouse, A., Gabernet-Castello, C., Field, M.C., and Dacks, J.B. (2012). Sculpting the endomembrane system in deep time: high resolution phylogenetics of Rab GTPases. J. Cell Sci. 125, 2500–2508. https://doi.org/10.1242/jcs.101378.

33. Klopper, T.H., Kienle, N., Fasshauer, D., and Munro, S. (2012). Untangling the evolution of Rab G proteins: implications of a comprehensive genomic analysis. BMC Biol. 10, 71. https://doi.org/10.1186/1741-7007-10-71.

34. Martin, S., Driessen, K., Nixon, S.J., Zerial, M., and Parton, R.G. (2005). Regulated localization of Rab18 to lipid droplets: effects of lipolytic stimulation and inhibition of lipid droplet catabolism. J. Biol. Chem. 280, 42325–42335. https://doi.org/10.1074/jbc.M506651200.

35. Dejgaard, S.Y., Murshid, A., Erman, A., Kizilay, O., Verbich, D., Lodge, R., Dejgaard, K., Ly-Hartig, T.B., Pepperkok, R., Simpson, J.C., et al. (2008). Rab18 and Rab43 have key roles in ER-Golgi trafficking. J. Cell Sci. 121, 2768–2781. https://doi.org/10.1242/jcs.021808.

36. Vazquez-Martinez, R., Cruz-Garcia, D., Duran-Prado, M., Peinado, J.R., Castano, J.P., and Malagon, M.M. (2007). Rab18 inhibits secretory activity in neuroendocrine cells by interacting with secretory granules. Traffic 8, 867–882. https://doi.org/10.1111/j.1600-0854.2007.00570.x.

37. Gronemeyer, T., Wiese, S., Grinhagens, S., Schollenberger, L., Satyagraha, A., Huber, L.A., Meyer, H.E., Warscheid, B., and Just, W.W. (2013). Localization of Rab proteins to peroxisomes: a proteomics and immunofluorescence study. FEBS Lett. 587, 328–338. https://doi.org/10.1016/j.febslet.2012.12.025.

38. Salloum, S., Wang, H., Ferguson, C., Parton, R.G., and Tai, A.W. (2013). Rab18 binds to hepatitis C virus NS5A and promotes interaction between sites of viral replication

and lipid droplets. PLoS Pathog. *9*. e1003513. https://doi.org/10.1371/journal.ppat.
1003513.

39. Gerondopoulos, A., Bastos, R.N., Yoshimura, S., Anderson, R., Carpanini, S.,
Aligianis, I., Handley, M.T., and Barr, F.A. (2014). Rab18 and a Rab18 GEF complex
are required for normal ER structure. J. Cell Biol. *205*, 707–720. https://doi.org/10.
1083/jcb.201403026.

40. Zeng, Y., and Cullen, B.R. (2002). RNA interference in human cells is restricted to the
cytoplasm. RNA *8*, 855–860. https://doi.org/10.1017/s1355838202020071.

41. Stalder, L., Heusermann, W., Sokol, L., Trojer, D., Wirz, J., Hean, J.,
Fritzsche, A., Aeschimann, F., Pfanzagl, V., Basselet, P., et al. (2013). The
rough endoplasmatic reticulum is a central nucleation site of siRNA-medi-
ated RNA silencing. EMBO J. *32*, 1115–1127. https://doi.org/10.1038/emboj.
2013.52.

42. Pepin, G., Perron, M.P., and Provost, P. (2012). Regulation of human Dicer by the
resident ER membrane protein CLIMP-63. Nucleic Acids Res. *40*, 11603–11617.
https://doi.org/10.1093/nar/gks903.